ISSN 1726-5479

# SENSORS & TRANSDUCERS

7 vol. 142 /12

## Sensor Networks and Wireless Sensor Networks

International Frequency Sensor Association Publishing

IFSA

# Sensors & Transducers

**Volume 142, Issue 7, July 2012** **www.sensorsportal.com** **ISSN 1726-5479**

Sensors & Transducers Journal (ISSN 1726-5479) is a peer review international journal published monthly online by International Frequency Sensor Association (IFSA).
Available in electronic and on CD. 

# Contents

Volume 142
Issue 7
July 2012

www.sensorsportal.com

ISSN 1726-5479

## Editorial Book Review



## Research Articles

Authors are encouraged to submit article in MS Word (doc) and Acrobat (pdf) formats by e-mail: editor@sensorsportal.com
Please visit journal's webpage with preparation instructions: http://www.sensorsportal.com/HTML/DIGEST/Submition.htm

International Frequency Sensor Association (IFSA).

*Sensors & Transducers Journal, Vol. 142, Issue 7, July 2012, pp. 76-86*

**Sensors & Transducers**
**ISSN 1726-5479**


# Theoretical Analysis to Capacitance of RF MEMS Clamped-Clamped Capacitive Switch

**Tian-Jie CAO**
The Airport College, Civil Aviation University of China, Tianjin 300300, China
Tel.: 86-022-24095061, fax: 86-022-24092470
E-mail: caotianjie@sohu.com

*Received: 2 May 2012 /Accepted: 23 July 2012 /Published: 31 July 2012*

**Abstract:** A one-dimensional three-stage static model for analyzing RF MEMS clamped-clamped capacitive switch was used to calculate the capacitance of the switch in the different states. This model is based on the small displacement assumptions of the clamped-clamped beam and divides the deformation of the clamped-clamped beam subjected to the electrostatic force into three stages: The first is a clamped-clamped beam subjected to electrostatic force without any constrain at the center; The second is a beam subjected to both a concentrated force and a moment and with a constraint at the center; The third is a beam subjected to both the electrostatic force and a concentrated force with a given displacement and a zero angle of rotation over the central part of the beam. With the model the capacitance of the switch in different states can be obtained and therefore the relation between the capacitance and the hold-on voltage and the relation between the capacitance and the contact region can be analyzed. From analysis the effect of some geometry dimensions, such as the length of the beam, the length of the pull-down electrode, the initial gap and the depth of the beam, on the capacitance can be understood and some conclusions may be useful to the design of the MEMS clamped-clamped capacitive switch. *Copyright © 2012 IFSA.*

**Keywords:** Capacitance, Clamped-clamped beam, Electrostatic force, RF MEMS switch.

## 1. Introduction

Since the first MEMS switch was reported by Petersen in 1979 [1], different kinds of MEMS switch have been developed by a number of companies and universities. These switches can be classified as direct metal-metal contact [2-4] or capacitive type [5-8].Among these MEMS switches, RF MEMS (Radio Frequency Micro Electro Mechanical Systems) capacitive switches show great potential for use in wireless communication and radar systems. Desirable aspects are low insertion loss, high isolation, and very low, near-zero power consumption. RF MEMS switches are the specific micro mechanical switches designed to operate at RF to mm-wave frequencies (0.1 to 100 GHz). The development of RF MEMS switches using metal membranes with capacitive coupling has also been reported [1-3]. Some theoretical calculation of insertion and isolation, which are two of the most important microwave parameters of a RF MEMS capacitive switch and primarily dominated by the switch capacitance, were presented[7].In the calculation, insertion is defined by a transmission coefficient in up-state, and isolation is defined by the coefficient in down-state. The switch capacitance in down-state contains two portions: the parallel-plate capacitance and the fringing capacitance, and the parallel-plate capacitance is only dependent on the area of the parallel-plate, the relative permittivity of the dielectric layer, and the depth of the dielectric layer, which is too simple to consider the effect of some geometry dimensions of a switch (such as the initial gap, the length of the switch beam, and so on) on the capacitance. In practice, because the determination of the contact area between the two plates is quite difficult and the contact area between the two plates cannot be expressed with a simple formula such as that in [7], in which the capacitance value is approximately given by the well-known parallel plate formula, the switch capacitance in down-state is quite different even to the same switch, depending on the actuation voltage and the structure of the switch. Therefore the isolation is not only dependent on frequencies but also dependent on actuation voltages and the structure of the switch. The behavior of electrically actuated microbeams has been studied using different models and approaches. Zavracky *et al.* [9] studied the static behavior of a cantilever microswitch by numerically solving the second-order differential equation of a beam and by using a spring-mass model. Chan *et al.* [10] utilized the finite-element package ABAQUS to study the static behavior of a fixed-fixed microbeam. Grtétillat *et al.* [11] studied the electromechanical behavior of asymmetric fixed-fixed microbeams using the MEMCAD system. Hung and Senturia [12] used a macromodel to simulate the dynamics of a fixed-fixed microbeam proposed as a pressure sensor. Soleymani et al. [13] used a distributed model to investigate the pull-in instability of circular plate subjected to nonlinear distributed electrostatic force using finite difference method. In this paper, a one-dimensional three-stage static model [14] for analyzing MEMS clamped-clamped capacitive switch is used to calculate the capacitance in the different states. With the model the relation between the capacitance and the hold-on voltage and the relation between the capacitance and the contact region are given in a graphic manner. From analysis the effect of some geometry dimensions on the capacitive can be understood and some conclusions may be useful to the design of a RF MEMS clamped-clamped capacitive switch.

## 2. Differential Equation of the Elastic Curve of the Beam

A typical capacitive RF MEMS switch is mainly composed by a clamped-clamped metal beam, the transmission line, and an insulator or dielectric layer fabricated on the transmission line [9], the side view of which is shown in Fig. 1. The mechanics model of the switch is shown in Fig. 2.

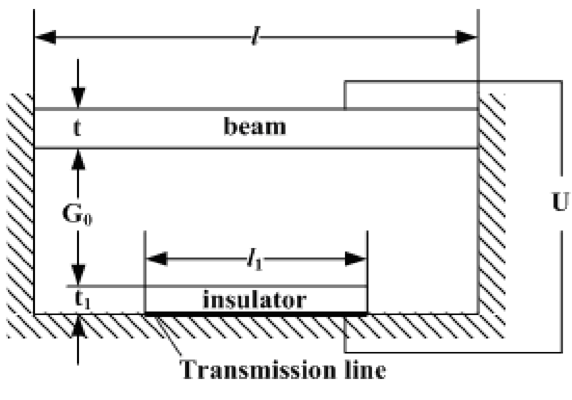


**Fig. 1.** Schematic diagram of a RF MEMS clamped-clamped capacitive switch.

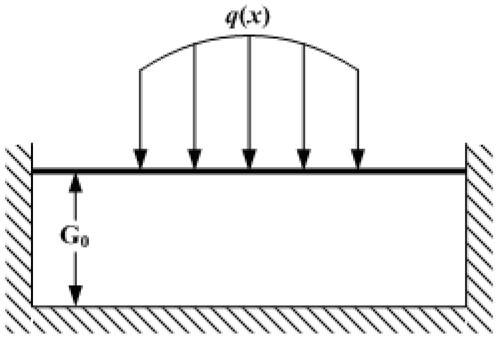


**Fig. 2.** Model of a clamped-clamped beam subjected to a load with constraint.

The beam and the dielectric length are *l and* $l_1$ respectively. The depth and width of rectangle cross-section of the beam are *t* and *B* respectively. The initial gap between the beam and the dielectric is $G_0$. The depth and width of the dielectric layer are $t_1$and *B* respectively. With the original point of the horizontal *x*-axial being at the center of the beam, the electrostatic force per unit length is

$$q(x) = \begin{cases} \frac{1}{2}\varepsilon_r\varepsilon_0 \frac{BU^2}{2(G - v(x))^2}, |x| < \frac{l_1}{2} \\ 0 \qquad , |x| \geq \frac{l_1}{2} \end{cases}, \tag{1}$$

where, $\varepsilon_0$ is the vacuum permittivity; $\varepsilon_r$ is the relative permittivity of the dielectric between the beam and the dielectric, if in air it is approximately equal to 1.0; *U* is the applied voltage; *v*(x) is the deflection at *x*; $G=G_0+t_1/\varepsilon_1$ is the initial equivalent gap between the two electrodes; $\varepsilon_1$ is the relative permittivity of the insulator.

The deformation of the clamped-clamped beam subjected to the electrostatic force as shown in Fig. 2 can be divided into three stages [14]: the first is a clamped-clamped beam only subjected to electrostatic force without any constrain at the center, and at the end of this stage the deflection at the central point reaches $G_0$; the second is a beam subjected to a concentrated force at the central point besides the electrostatic force with a constraint at the center, and at the end of the second stage the moment at the central point is zero; the third is a beam subjected to both the electrostatic force and a concentrated force with a given displacement and a zero angle of rotation over the central part of the beam.

Suppose the small displacement assumptions are applicable and the clamped-clamped beam is a symmetrical one. As a result the half of the beam can be seen a cantilever beam, in which the free end of the cantilever beam with zero angle of rotation is the central point of the clamped-clamped beam. Taking the right half of the clamped-clamped beam for example, the deformation and the loads are shown in Fig. 3.

The elastic curve of the beam in Fig. 3 is governed by the fourth-order non-linear differential equation,

$$\frac{d^4 v}{dx^4} = \frac{q(x)}{D} \tag{2}$$

where， $D = \frac{Bt^3}{12}\frac{E}{1-\mu^2}$， $E$ is the Young's modulus or modulus of elasticity of the beam， $\mu$ is the Poisson's ratio

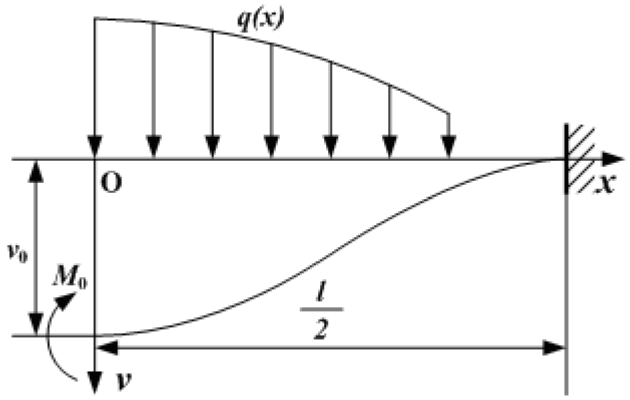


**Fig. 3.** Cantilever beam subjected to the loads at 1st stage.

## 3. Calculation of the Capacitance at Different Stages

The insertion loss and isolation dominated primarily by the switch capacitance are two of the most important microwave parameters of a RF MEMS switch. They are both defined by transmission coefficient $S_{21}$: insertion loss is $|S_{21}|$ in up-state, while isolation is $|S_{21}|$ in down-state [11]. In the paper we focus only on the calculation of the switch capacitance because of its key role in calculation of the insertion and isolation.

### 3.1. Capacitance at the First Stage

If the boundary conditions at the free end of the cantilever beam can be obtained in any state. The deflection at any cross section then can be obtained numerically from the equation (2). The boundary conditions of the differential equation (2) at the free end are

$$\begin{aligned} & v(0) = v_0, \frac{dv(0)}{dx} = 0 \\ & \frac{d^2v(0)}{dx^2} = -\frac{M_0}{D}, \frac{d^3v(0)}{dx^3} = 0 \end{aligned}, \tag{3}$$

where, the moment $M_0$ and the deflection $v_0$ at the free end are unknown, or the moment $M_0$ at the free end and the applied voltage $U$ are unknown ($v_0$ must be given because the beam is not controllable on the voltage reaching the pull-in voltage). They can be obtained with a two-fold method of bisection from the conditions that both the deflection and the slope at the fixed end are zero (the detail can be seen in [14], although the model in [14] is for a direct metal-metal contact type MEMS switch and the formula of the electrostatic force per unit length is slightly different). Obtaining the deflection $v(x)$ at any cross section and considering symmetry of the switch, one can calculate the capacitance of the switch numerically as follows [12],

$$C_{1\mathrm{st}} = 2\varepsilon_0\varepsilon_r \int_0^{l/2} \frac{Bdx}{G - v(x)} \tag{4}$$

The fringing capacitance is neglected in equation (4).

### 3.2. Capacitance at the Second Stage

At the beginning of this stage the deflection at the central point reaches $G_0$, while at the end of the second stage the moment at the central point is zero. At the stage, the beam is subjected to a concentrated force at the central point besides the electrostatic force because of the constraint at the center. The deformation of the beam subjected to the loads is shown in Fig. 4.

Suppose the applied voltage is $U$, the boundary conditions of the differential equation (2) at the free end are

$$v(0) = G_0, \frac{dv(0)}{dx} = 0$$
$$\frac{d^2v(0)}{dx^2} = -\frac{M_0}{D}, \frac{d^3v(0)}{dx^3} = -\frac{Q_0}{D} \quad (5)$$

where, the shearing force $Q_0$ and the moment $M_0$ at the free end are unknown. They can be obtained in a similar way from the conditions that both the deflection and the slope at the fixed end are zero. Similar to the first stage, the capacitance is

$$C_{2\text{nd}} = 2\varepsilon_0\varepsilon_r \int_0^{l/2} \frac{Bdx}{G - v(x)} \quad (6)$$

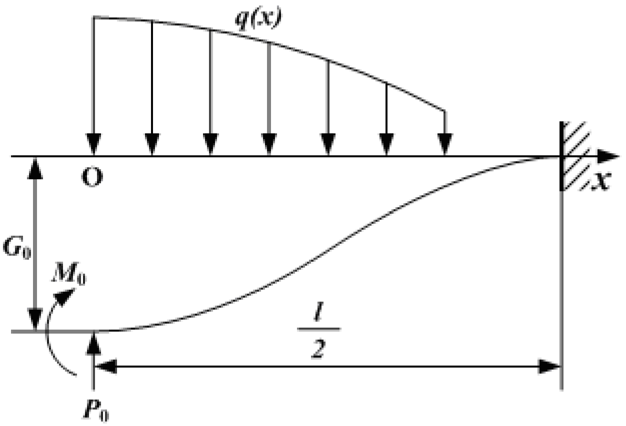


**Fig. 4.** Cantilever beam subjected to the loads at 2nd stage.

### 3.2. Capacitance at the Third Stage

Supposing the contact between the beam and the dielectric is smooth and there is no gap when they are contacted .At this stage the deflection over the central part Δ of the beam reaches $G_0$, and there is no moment or shearing force over the contact region because of the balance between the reaction and the electrostatic force over the contact region. The deformation of the beam subjected to the loads at the third stage is shown in Fig. 5.

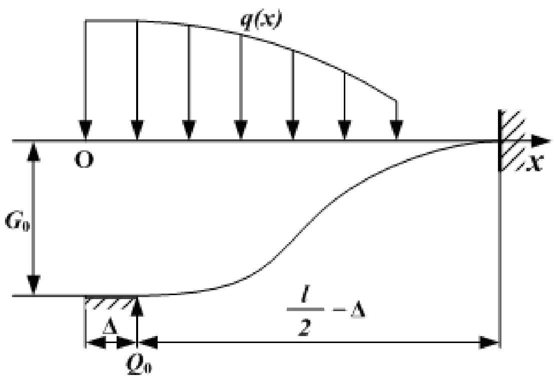


**Fig. 5.** Cantilever beam subjected to the loads at 3rd stage.

Suppose the applied voltage is $U$, the boundary conditions of the differential equation (2) at $x$=Δ are

$$\begin{aligned} v(\Delta) = G_0, \frac{dv(\Delta)}{dx} = 0 \\ \frac{d^2v(\Delta)}{dx^2} = 0, \frac{d^3v(\Delta)}{dx^3} = -\frac{Q_0}{D} \end{aligned} \tag{7}$$

At the stage, the shearing force $Q_0$ and the contact length Δ are unknown. They can also be obtained from the conditions that both the deflection and the slope at the fixed end are zero. The capacitance then can be calculated numerically as follows

$$C_{3\mathrm{rd}} = 2\varepsilon_0\varepsilon_r\left[\frac{\varepsilon_1 B\Delta}{t_1} + \int_{\Delta}^{l/2}\frac{Bdx}{G - v(x)}\right] \tag{8}$$

## 4. Examples

### 4.1. Example 1

In this example, a general analysis will be made. The material and geometrical parameters in the example are shown in Table 1.

**Table 1.** Material and Geometrical Parameters.

| Symbol | Quantity | Value |
|---|---|---|
| $E$ | Modulus of elasticity of the beam | 76.52 Gpa |
| $\mu$ | Poisson's ratio of the beam | 0.41 |
| $\varepsilon_0$ | Vacuum permittivity | $8.854\times10^{-12}$ F·m$^{-1}$ |
| $\varepsilon_1$ | Relative permittivity of the insulator | 7.6 |
| $\varepsilon_r$ | Relative permittivity of air | 1.0 |
| $B$ | Width of the beam | 90 μm |
| $t$ | Depth of the beam | 1.5 μm |
| $l$ | Length of the beam | 280 μm |
| $l_1$ | Length of the insulator | 200 μm |
| $t_1$ | Thickness of the insulator | 0.15 μm |
| $G_0$ | The initial gap | 1.5 μm |

One can solve the differential equation (2) under boundary conditions at the three different stages and calculate the capacitance depending on the applied voltage. The relation between the capacitance and the applied voltage is shown in Fig. 6. The applied voltage at the end of the first stage is about 1.40 V, and the corresponding capacitance is about 1.20 pF. At the end of the second stage they are about 3.87 V and 1.50 pF, respectively. The pull-in voltage of the switch is about 15.47 V, to which two capacitances 0.15 pF at deflection $v_0$=0.59 μm of the first stage and 6.35 pF at contact length Δ=69.63 μm of the third stage are corresponding. The relation between applied voltage and the contact length at the third stage is shown in Fig. 7. It can be seen from Fig. 7 that the pull-in voltage cannot give the maximum contact area, which is required for the maximum capacitance of a MEMS switch. Under different hold-on voltages, which are the applied voltage to maintain a RF MEMS switch in down-state, there are different capacitances unlike a parallel-plate capacitance. So the isolation of a RF MEMS switch is not only dependent on the frequency of a signal but also dependent on the hold-on voltage applied to the switch, and because the capacitance increases much more quickly at the third stage than the first two stages with the applied voltage increasing, the isolation may be quite different from one down-state to another.

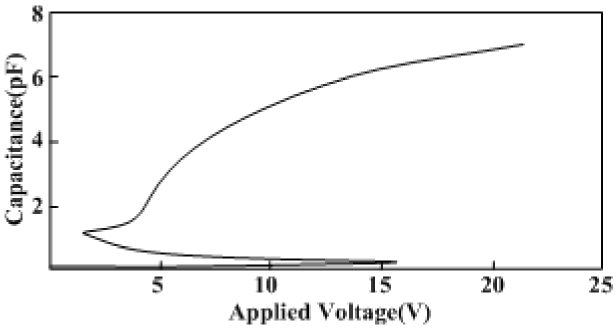


**Fig. 6.** Relation between applied voltage and capacitance.

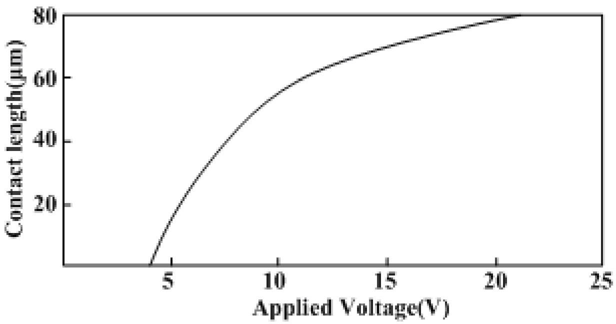


**Fig. 7.** Relation between applied voltage and contact length.

### 4.2. Example 2

In this example, the effect of some geometry dimensions, the length of the beam, the length of the pull-down electrode(that is the length of the transmission line), the initial gap and the depth of the beam, on the capacitance of the RF MEMS switch under a special hold-on voltage—pull-in voltage—will be analyzed. Note please that in the example, all parameters are the same as the Table 1 except for the geometry dimension under discussion. The relation between the length of the clamped-clamped beam and the pull-in voltage is shown in Fig. 8, and the relation between the length of the beam and the capacitance is shown in Fig. 9. The relation between the length of the pull-down electrode and the pull-in voltage is shown in Fig. 10, and the relation between the length of the pull-down electrode and the capacitance is shown in Fig. 11. The relation between the initial gap between the beam and the dielectric and the pull-in voltage is shown in Fig. 12, and the relation between the initial gap and the capacitance is shown in Fig. 13. The relation between the depth of the beam and the pull-in voltage is shown in Fig. 14. The relation between the depth of the beam and the capacitance is omitted because it is a horizontal line (the capacitance is about 6.35 pF, and the contact length is about 69.63 μm).

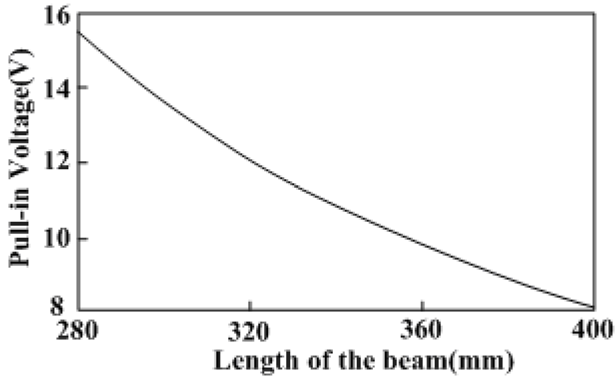


**Fig. 8.** Relation between length of the beam and pull-in voltage.

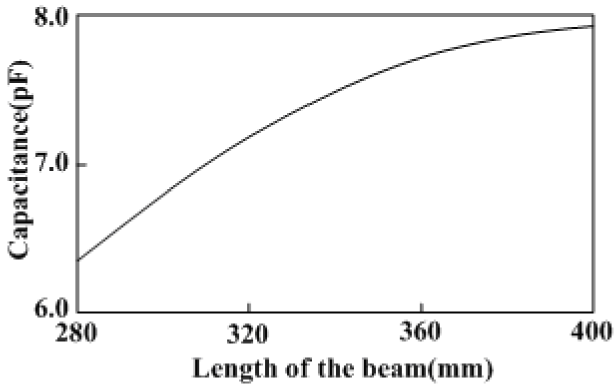


**Fig. 9.** Relation between length of the beam and capacitance.

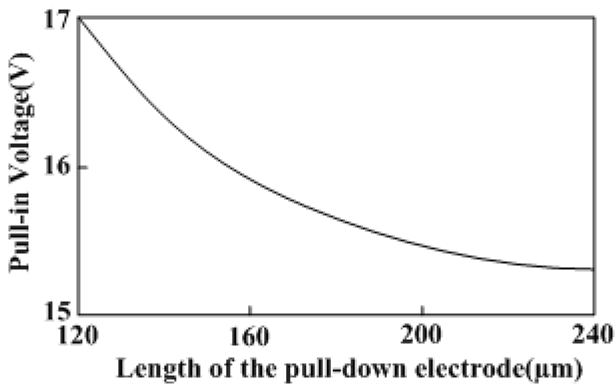


**Fig. 10.** Relation between length of pull down electrode and pull-in voltage.

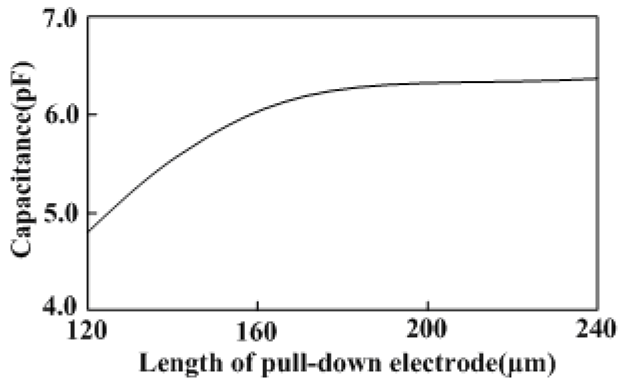


**Fig. 11.** Relation between length of pull down electrode and capacitance.

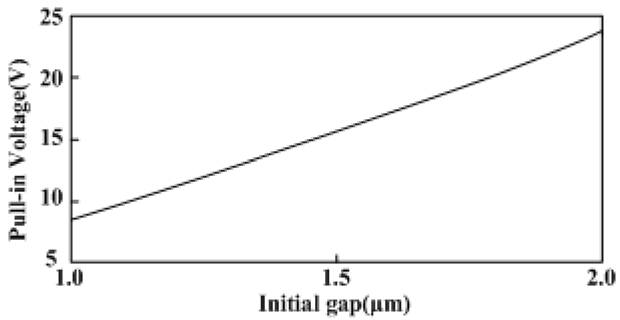


**Fig. 12.** Relation between the initial gap and pull-in voltage.

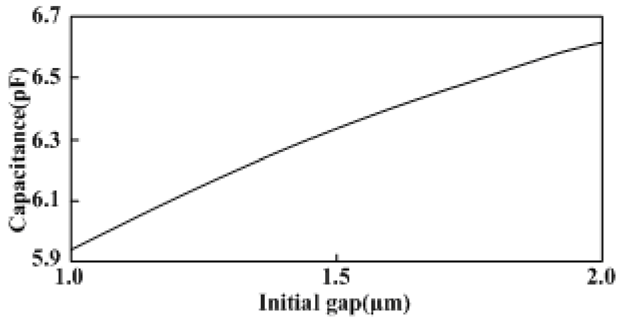


**Fig. 13.** Relation between the initial gap and capacitance.

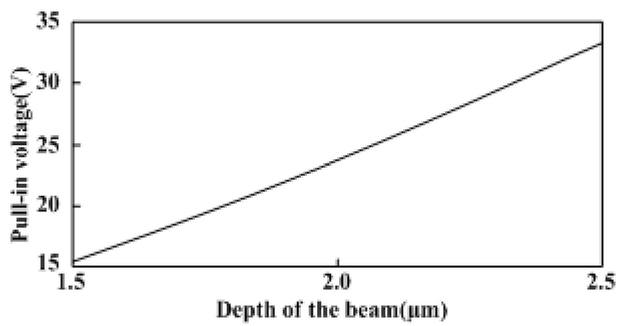


**Fig. 14.** Relation between depth of the beam and pull-in voltage.

It is found from Fig. 8 and Fig. 9 that increase in the length of the beam will decrease the pull-in voltage and increase the capacitance corresponding to the pull-in voltage; we can observe from Figs. 10 and 11 that the pull-in voltage will decrease and the capacitance increase with increase in the length of the pull-down electrode, but the capacitance increases quite slow after the length of the pull-down electrode is longer than 160 µm; we can also observe from Figs. 12 and 13 that the increase in the initial gap has significant effect on the pull-in voltage and the capacitance corresponding to the pull-in voltage; increases in the depth of the beam show that the pull-in voltage will increase with the increase in the depth of the beam significantly but no change in the capacitance corresponding to the pull-in voltage is found.

## 5. Conclusions

In this paper a one-dimensional three-stage static model for analyzing RF MEMS clamped-clamped capacitive switch is used to calculate the capacitance of the switch in the different down-states. With the model capacitances of the switch in different states are obtained, and therefore the relation between the contact length and the hold-on voltage and the relation between the capacitance and the hold-on voltage are analyzed. In addition, the effect of some geometry factors on the capacitance corresponding to the pull-in voltage is analyzed. From the analysis the effect of hold-on voltage, the length and depth of the beam, the initial gap, and the length of the transmission line of a RF MEMS switch on the capacitance can be understood, which may be useful to the design of the MEMS clamped-clamped capacitive switch. From the view point of the capacitance of a RF MEMS switch, the hold-on voltage is more important than pull-in voltage because it is the hold-on voltage that determines the capacitance of a RF MEMS switch, so one should carefully select hold-on voltage according to the requirement to the capacitance of a RF MEMS switch based on the requirement to the isolation of a RF MEMS switch and frequency of the signal.

## References


[1]. K. E. Petersen, Micromechanical membrane switches on silicon, *IBM Journal of Research and Development archive*, Vol. 23, Issue 4, 1979, pp. 376-385.

[2]. S. Majumder, N. E. McGruer, P. M. Zavracky, G. G. Adams, R. H. Morrison, J. Krim, Measurement and modeling of surface micromachined, electrostatically actuated microswitches, in *Proceedings of the International Conference on Solid-state Sensors and Actuators*, Chicago, USA, June 16-19, 1997, pp. 1145-1148.

[3]. Y. Wang, Z. H. Li, D. T. McCormick, N. C. Tien, Low-voltage lateral-contact microrelays for RF applications, in *Proceedings of the 15$^{th}$ IEEE International Conference on Micro Electro Mechanical Systems*, Las Vegas, NV, USA, 20-24 January 2002, pp. 645-648.

[4]. Y. Shi, S-G. Kim, A lateral, self-cleaning, direct contact MEMS switch, in *Proceedings of the 18$^{th}$ IEEE International Conference on Micro Electro Mechanical Systems*, Miami Beach, Florida, USA, 30 January - 3 February 2005, pp. 195-198.

[5]. C. Goldsmith, T. H. Lin, B. Powers, R. W. Wen, B. , Norvell, Micromechanical membrane switches for microwave applications, in *Proceedings of the Microwave Symposium Digest, 1995, IEEE MTT-S International*, Orlando, FL , USA, 16-20 May, 1995, pp. 91-94.

[6]. M. Daneshmand, R. R. Mansour, C-type and R-type MEMS switches for Redundancy Switch Matrix applications, in *Proceedings of the Microwave Symposium Digest, 2006, IEEE MTT-S International*, San Francisco, CA, USA, 11-16 June, 2006, pp. 144-147.

[7]. K. Chen, Y. Y Dai, X. D Zou, J. W. Zhang, A low-loss RF MEMS switch with dielectric layer on the lower surface of the bridge, in *Proceedings of the 4$^{th}$ IEEE international Conference on Nano/Micro Engineered and Molecular Systems*, Shenzhen, China, January 5-8, 2009, pp. 152-155.

[8]. C. L. Goldsmith, Z. M Yao, S. S Eshelman, D. Denniston, Performance of low-loss RF MEMS capacitive switches, *IEEE Microwave and Guided Wave Letters*, Vol. 8, Issue 8, 1998, pp. 269-271.

[9]. P. M. Zavracky, S. Majumder, and N. E. McGruer, Micromechanical switches fabricated using nickel surface micromachining, *Journal of Microelectromechanical System*, Vol. 6, Issue 1, 1997, pp. 3–9.
[10]. E. K. Chan, K. Garikipati, and R. W. Dutton, Characterization of contact electromechanics through capacitance-voltage measurements and simulations, *Journal of Microelectromechanical System*, Vol. 8, Issue 2, 1999, pp. 208–217.
[11]. M. A. Grtétillat, Y. J. Yang, E. S. Hung, V. Rabinovich, G. K. Ananthasuesh, N. F. Rooij, and S. D. Senturia, Nonlinear electromechanical behavior of an electric microrelay, in *Proceedings of the International Conference on Solid-state Sensors and Actuators*, Chicago, USA, June 16-19, 1997, pp. 1141-1144.
[12]. E. S. Hung and S. D. Senturia, Generating efficient dynamical models for microelectromechanical systems from a few finite-element simulations runs, *Journal of Microelectromechanical System*, Vol. 8, Issue 3, 1999, pp. 280-289.
[13]. P. Soleymani, H. Sadeghian, A. Tahmasebi, G. Rezazadeh, Pull-in Instability Investigation of Circular Micro Pump Subjected to Nonlinear Electrostatic Force, *Sensors & Transducers,* Vol. 69, Issue 7, 2006, pp. 622-628.
[14]. T. J. Cao, F. Ding, Static Analysis Model of Micro-machined Switch Consisting of Clamped-Clamped Beam, *Engineering Mechanics*, Vol. 23, Issue 9, 2006, pp. 42-47, 54 (in Chinese).

# Guide for Contributors

## Aims and Scope

*Sensors & Transducers Journal (ISSN 1726-5479)* provides an advanced forum for the science and technology of physical, chemical sensors and biosensors. It publishes state-of-the-art reviews, regular research and application specific papers, short notes, letters to Editor and sensors related books reviews as well as academic, practical and commercial information of interest to its readership. Because of it is a peer reviewed international journal, papers rapidly published in *Sensors & Transducers Journal* will receive a very high publicity. The journal is published monthly as twelve issues per year by International Frequency Sensor Association (IFSA). In additional, some special sponsored and conference issues published annually. *Sensors & Transducers Journal* is indexed and abstracted very quickly by Chemical Abstracts, IndexCopernicus Journals Master List, Open J-Gate, Google Scholar, etc. Since 2011 the journal is covered and indexed (including a Scopus, Embase, Engineering Village and Reaxys) in Elsevier products.

## Topics Covered

Contributions are invited on all aspects of research, development and application of the science and technology of sensors, transducers and sensor instrumentations. Topics include, but are not restricted to:

- Physical, chemical and biosensors;
- Digital, frequency, period, duty-cycle, time interval, PWM, pulse number output sensors and transducers;
- Theory, principles, effects, design, standardization and modeling;
- Smart sensors and systems;
- Sensor instrumentation;
- Virtual instruments;
- Sensors interfaces, buses and networks;
- Signal processing;
- Frequency (period, duty-cycle)-to-digital converters, ADC;
- Technologies and materials;
- Nanosensors;
- Microsystems;
- Applications.

## Submission of papers

Articles should be written in English. Authors are invited to submit by e-mail editor@sensorsportal.com 8-14 pages article (including abstract, illustrations (color or grayscale), photos and references) in both: MS Word (doc) and Acrobat (pdf) formats. Detailed preparation instructions, paper example and template of manuscript are available from the journal's webpage: http://www.sensorsportal.com/HTML/DIGEST/Submition.htm Authors must follow the instructions strictly when submitting their manuscripts.

## Advertising Information

Advertising orders and enquires may be sent to sales@sensorsportal.com Please download also our media kit: http://www.sensorsportal.com/DOWNLOADS/Media_Kit_2012.pdf